



Original Research Article

# Enhanced Photocatalytic Removal of Direct Yellow 50 by ZnO/MWCNTs Nanocomposite under Solar Light Irradiation through Response Surface Methodology (RSM) Optimization

Resan Abdulamer<sup>1\*</sup>, Thura Zayad Fathallah<sup>2</sup> , Ruaa Sattar<sup>3</sup>, Youssef Ali Naeem<sup>4</sup> , Ameer Hassan Idan<sup>5</sup> , Hussein Ali Kadhim Kyhoiesh<sup>6</sup> , Yassir Mohammed Nasr<sup>7</sup>

<sup>1</sup>Department of Medical Laboratories Technology, Al-Nisour University College, Baghdad, Iraq

<sup>2</sup>Department of Pharmaceutics, College of Pharmacy, Al-Noor University, Bartella, Iraq

<sup>3</sup>Department of Pharmacy, Al-Hadi University College, Baghdad, Iraq

<sup>4</sup>Department of Pharmacy, Al-Manara College for Medical Sciences, Maysan, Iraq

<sup>5</sup>Department of Pharmacy, Al-Zahrawi University College, Karbala, Iraq

<sup>6</sup>College of Health and Medical Technology, National University of Science and Technology, Dhi Qar, Iraq

<sup>7</sup>Department of Pharmacy, Mazaya University College, Annasiriyah, Iraq

## ARTICLE INFO

### Article history

Submitted: 02 June 2024

Revised: 12 July 2024

Accepted: 20 July 2024

ID: [AJCA-2407-1580](https://doi.org/10.48309/AJCA.2025.465609.1580)

DOI: [10.48309/AJCA.2025.465609.1580](https://doi.org/10.48309/AJCA.2025.465609.1580)

### KEYWORDS

Co-doping

Orange G

Photodegradation

Sol-gel method

Cu-Mg-TiO<sub>2</sub>

## ABSTRACT

Photocatalytic degradation of direct yellow 50 dye DY from aqueous solution utilizing ZnO/MWCNTs nanocomposite under irradiation of solar light was studied in the proposed study. ZnO/MWCNTs nanocomposite was initially synthesized via hydrothermal method. The integration of MWCNTs into ZnO NPs structure resulted in increased roughness and porosity, thereby improving active sites onto nanocomposite, which can enhance effective surface area and also can be characterized via different techniques, such as FESEM, TEM, and BET. Response surface methodology (RSM) approach was used in this study. Several factors such as nanocatalyst quantity and concentration of DY dye were best the optimal conditions to examine the best degradation capacity for DY dye with solar light source. In this regard, the best degradation capacity was observed at 0.3 g of ZnO/MWCNTs nanocomposite for concentration 30 mg/L at 25 °C with 1 h irradiation time. Photocatalytic degradation was completed after 60 minutes of solar light irradiation, 93.56 % degradation efficiency of DY dye was also obtained. Thus, capability of nanocomposite was appeared to remove DY dye from wastewater. As a result, successfully syntheses a new form of ZnO nanoparticles embedded with MWCNTs. ZnO/MWCNTs, which may be utilized photocatalytic degradable of DY dye. According to the degradation results, DY dye might be effectively degradation from aqueous solutions utilizing ZnO/MWCNTs nanocomposite.

\* Corresponding author: Abdulamer, Resan

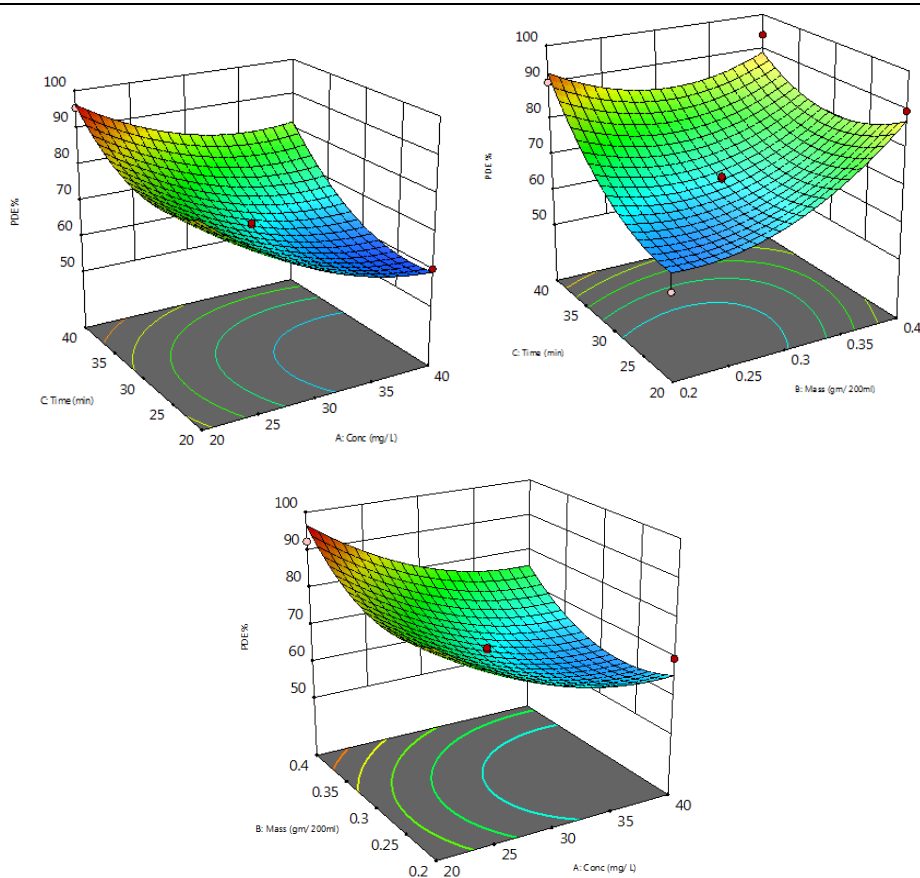
✉ E-mail: [abdulamerresan@gmail.com](mailto:abdulamerresan@gmail.com)

© 2025 by SPC (Sami Publishing Company)

---

**GRAPHICAL ABSTRACT**


---


**Introduction**

In recent years, environmental pollution resulting from the rapid development of industries has become a cause of widespread concern, as pollutants threaten human life and must be declined. One of the most dangerous pollutants is dyes which ranks third among the common toxic and dangerous pollutants found in wastewater, including dye production, leather tanning, printing, pharmaceuticals, textiles, dyeing, and pollution, urgent metal plating, electrical appliances, or electronic equipment, and so on. Meanwhile, among the most toxic organic pollutants, the concentration of dye in safe drinking water is less than 0.05 mg/L. It has a very high ability to dissolve in water and a carcinogenic effect, and easily penetrates the body through digestion, skin, mucous

membranes, and the respiratory system, causing great harm to living organisms [1-3]. Excessive exposure to dyes may cause acute toxicity, genetic mutations, and carcinogenic diseases, pulmonary congestion, and stomach ulcer inflammation. Dye was a precious heavy metal and is considered as a raw material used in many alloys and for hardening steel and also producing stainless steel [4-6]. Dye plating is used to obtain steel with mirror polished quality, hardness and aesthetics and to improve corrosion resistance. Dye is used as industrial catalysts, printing inks and pigments, glass, copper dyeing, and cement [7-10]. Direct yellow DY dye powder is soluble in water and sufficiently soluble in ethanol to lemon yellow, slightly soluble in acetone and strong sulfuric acid, and utilized for dyeing viscose and cotton. Dead cotton has a certain covering strength and it can also be utilized for printing

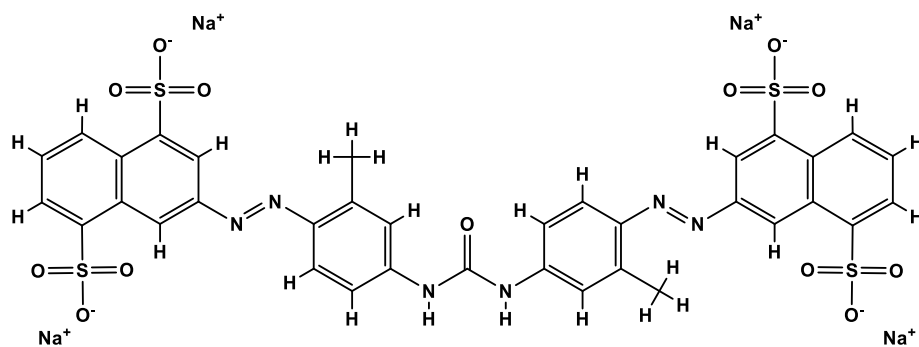


**Figure 1.** Chemical structure of direct yellow 50 DY dye.

viscose fabrics or cotton, wool, silk, polyamide fiber, and blended fabric dyeing. Likewise, it can be utilized for leather, biological shading, and paper, and its heavy metal salt can be used in pigment. Chemical structure of direct yellow 50 DY dye is displayed in Figure 1 [11,12]. In this study, ZnO/MWCNTs nanocomposite were fabricated through free-template and one-step synthesis by hydrothermal method introducing ZnO on the MWCNTs. The physical and optical properties of ZnO/MWCNTs nanocomposite were studied via several characterizations. The photo catalytic possessions of ZnO/MWCNTs nanocomposite were utilized for removal of DY dye from aqueous solution.

## Materials and Methods

### Preparation of nanocomposite

A hydrothermal method was useful to prepared ZnO/MWCNTs nanocomposite as the following method. 8 g in 50 mL of oxalic acid (Sigma-Aldrich), 99.0%, 10 g in 50 mL of zinc acetate (Sigma-Aldrich), 99.0%, was added to stir for obtaining a white homogeneous suspension. The white homogeneous suspension was then added to 0.04 g in 5 mL of MWCNTs which was acquired from the refinery of bakery factories magnetically agitated for 1 h. The suspension was then placed in 250 ml and heated to 150 °C

for 24 h. The bulk powder cooling, collected, and washed by distilled water. The powder was dried at 65 °C for 24 h.

## Result and Discussion

### Characterization

The pore structure, pore size distribution, and surface area of ZnO/MWCNTs were determined using the BET technique in the presence of nitrogen. The isotherm of ZnO/MWCNTs shows a small hysteresis loop that can be classified as kind IV. The average pore diameter, surface area, and total pore volume were calculated after incorporating carbon nanotubes into grafted zinc oxide. Interfacial interactions between carbon nanotubes and zinc oxide have an important influence on the structure and pore diameter of the material [13], as depicted in Figure 2.

The FE-SEM technique was used as an important and basic method to characterize the surface morphology and basic physical properties of the adsorbent. The zinc oxide nanoparticles were arranged in a spherical pattern in the form of random, disordered white balls. These pores provided a strong opportunity for the zinc oxide nanoparticles to entangle within them (Figure 3a). FESEM image was also used to characterize the surface morphology of MWCNT [14].

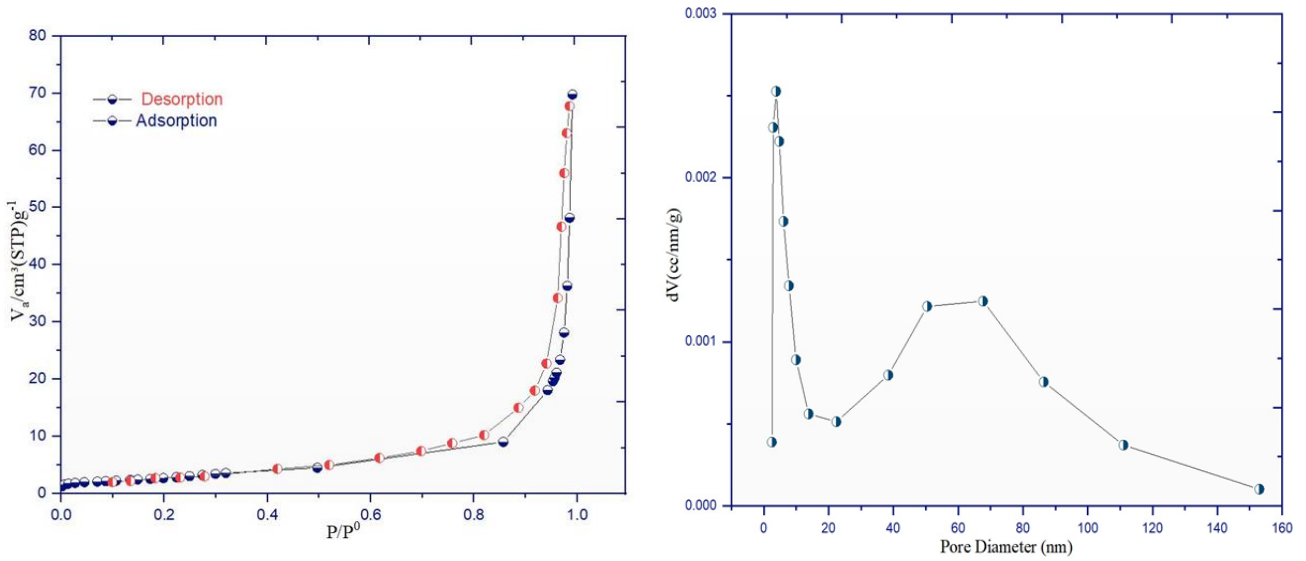


Figure 2. BET technique of ZnO/MWCNTs.

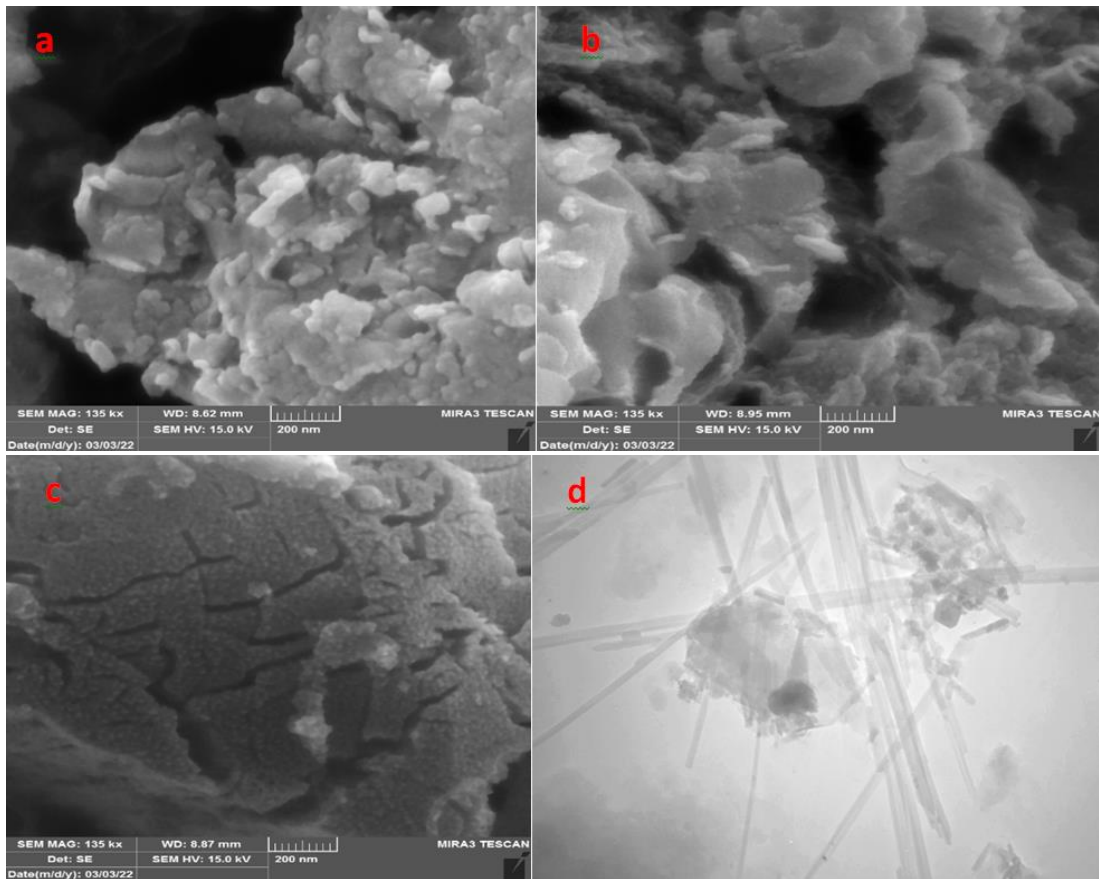


Figure 3. FESEM image of a) ZnO NPs, b) MWCNT, c) ZnO/MWCNTs, and TEM image of d) ZnO/MWCNTs.

It is evident from (Figure 3b) that the MWCNTs are cylindrical, curved, and tangled together. Microscopic images of carbon nanotubes show

that the rough porous surface showed phase changes due to the presence of new irregular macromolecules on the surface. This leads to an

increase in the prominence of the surface texture and its roughness as (Figure 3c) [15,16].

The surface morphology of ZnO/MWCNTs nanocomposites was studied using TEM technology. It was clear from the figure that the surface had a geometric shape resulting from cloud-like clusters with the presence of irregular agglomerations, resulting from the grafting of the surface with zinc oxide. Here the role of carbon on the surface of zinc oxide in explaining the increase in surface area becomes clear surface of the nanocomposite [17,18].

#### Experimental design via RSM approach

A design expert software version 13 was used. In experimental design via the response surface methodology (RSM) approach, a CCD approach was used to achieve the minimum required experimental runs. A second-order model was obtained in this approach [19]. Fractional

factorial design approach studies the main and a minimum number of experiments doing for interaction effects [20]. Some coded and actual values of variables are listed in Table 1. The true regression can be recognized as the value of the adjusted R-squared ( $R^2_{adj}$ ) and the coefficient of determination ( $R^2$ ). Although the new elements added to the model are meaningful, the high  $R^2$  values do not make the model valid for predicting new observations.  $R^2_{adj}$  is introduced for this case and increases as time increases to develop the model. The presence of inappropriate content in the sample reduces  $R^2_{adj}$ . Another term is  $R^2_{pred}$ , which indicates the model's ability to predict new responses and model over-fitting. Correlation coefficients  $R^2 = 0.9513$ , adjusted  $R^2 = 0.8886$  close to 1, estimated  $R^2$  (pred  $R^2$ ) = 0.2284 close to zero, confirming that the model is good for testing but too little for prediction.

**Table 1.** The coded and actual values as well as ANOVA results obtained RSM study of DY photocatalytic degradation by the prepared ZnO/MWCNT catalyst

Selected Variables								
Factor	Name	Units	Minimum	Maximum	Coded Low	Coded High	Mean	Std. Dev.
A	Conc.	mg/L	20.00	40.00	-1 ↔ 20.00	+1 ↔ 40.00	30.00	7.07
B	Mass	gm	0.200	0.400	-1 ↔ 0.20	+1 ↔ 0.40	0.300	0.078
C	Time	min.	20.00	40.00	-1 ↔ 20.00	+1 ↔ 40.00	30.00	7.07
ANOVA Results								
Source	Sum of Squares	df	Mean Square	F-value	p-value			
Model	2562.38	9	284.71	15.18	0.0008			
A-Conc	830.08	1	830.08	44.27	0.0003			
B-Mass	236.31	1	236.31	12.60	0.0093			
C-Time	540.38	1	540.38	28.82	0.0010			
AB	0.3025	1	0.3025	0.0161	0.9025			
AC	36.06	1	36.06	1.92	0.2081			
BC	210.54	1	210.54	11.23	0.0122			
A <sup>2</sup>	142.68	1	142.68	7.61	0.0282			
B <sup>2</sup>	244.08	1	244.08	13.02	0.0086			
C <sup>2</sup>	248.75	1	248.75	13.27	0.0083			
Residual	131.25	7	18.75					
Lack of Fit	129.76	3	43.25	115.96	0.0002			
Pure Error	1.49	4	0.3730					
Cor Total	2693.64	16						

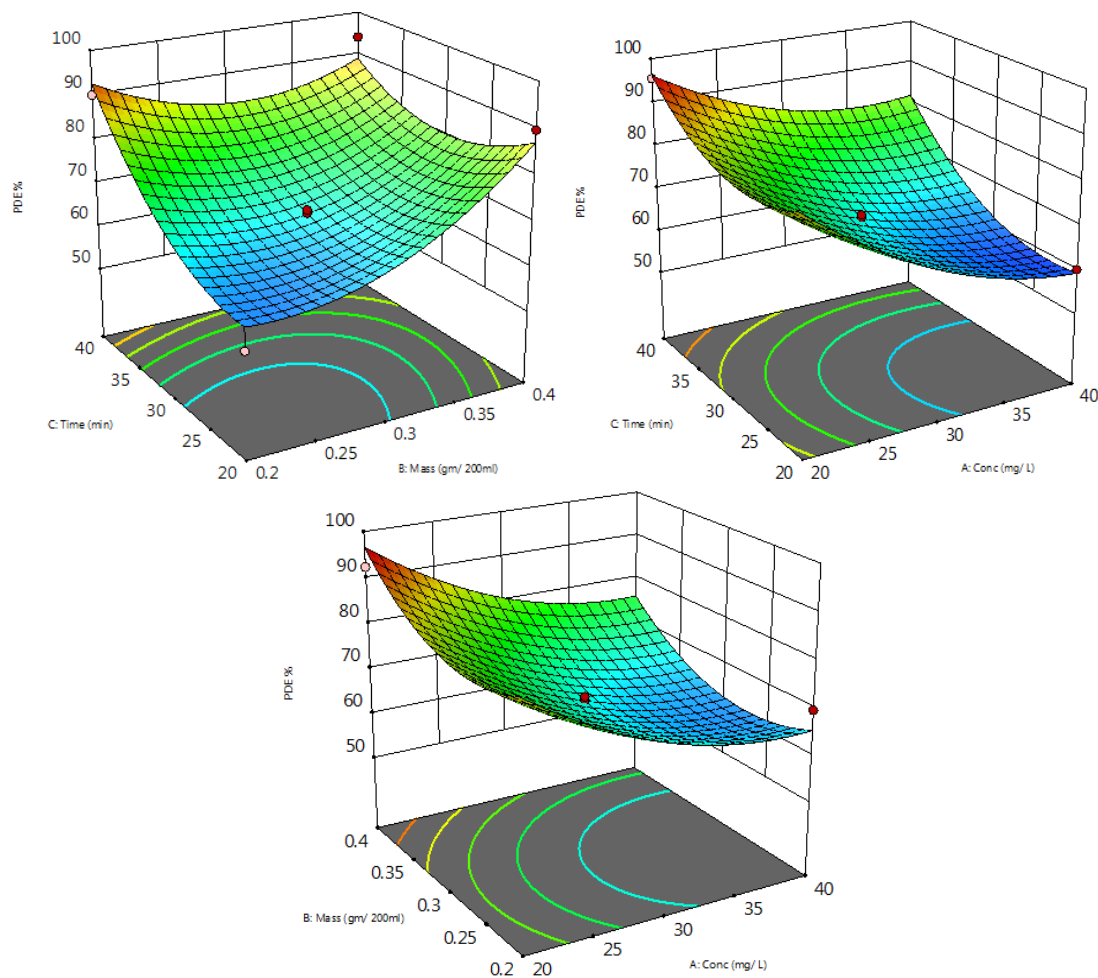


**Figure 4.** 3D plot surface and 2D contour plot of the photo-degradation of DY on the surface of ZnO/MWCNT surface.

### Model graph

The 3D response surface obtained in DY photodegradation is depicted in [Figure 4](#) together with the corresponding 2D contour plot in ZnO/MWCNT. The efficiency of the e/h splitter depends on the ratio of connected electronic components; the maximum photodegradation rate of the dye was determined as 95.45%, three-dimensional space surface. The maximum photodegradation efficiency is 99.45%. [Figure 4\(c\)](#) shows a three-dimensional response surface constructed to illustrate the effect of two variables (catalyst amount and dye concentration) on photodegradation efficiency.

The BPA degradation is mainly affected by the catalyst compared to the initial concentration.

### Effect of weight of ZnO/MWCNTs

The influence weight of ZnO/MWCNTs on photocatalytic degradation of DY dye was studied using 30 mg/L, flow rate of air 10 mL/min at 25 °C. When the weight of ZnO/MWCNTs increases, the photo catalytic degradation of DY dye increases until it reaches 0.3 g /200 mL, as shown in [Figure 5](#). The ZnO/MWCNTs has the efficiency to absorb the most light. Thus, 0.3 g of ZnO/MWCNTs gives the best photo degradation capacity because increased amount of photon of light cases leads to the degradation of DY dye.

However, at 0.1 g of ZnO/MWCNTs a reduction was experienced in photo degradation capacity [21-23]. The photo catalytic degradation PDE% of DY dye degradation occurred against the multiple quantities of ZnO/MWCNTs. The photo catalytic activity of the modified ZnO/MWCNTs rises with increasing weight of ZnO/MWCNTs from 0.1-0.4 g/200 mL. This indicates that the active site provided for substrate adsorption on the surface is limited to the quantity of 0.3 g/200 mL ZnO/MWCNTs. because the active sites are consumed via ZnO/MWCNTs during reactions that delay further photo catalytic degradation as show in Figure 6.

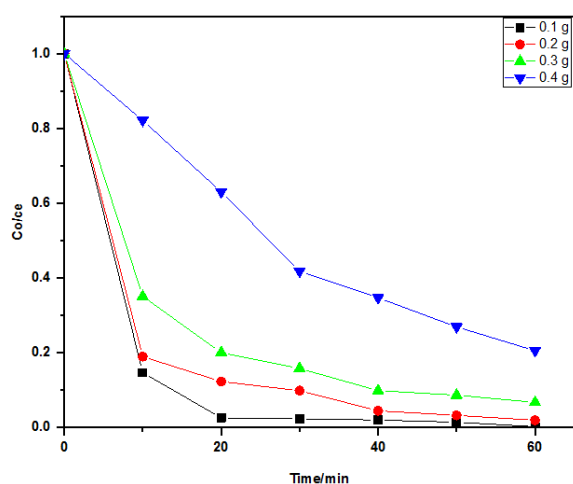


Figure 5. Photocatalytic activity of DY dye at different weights of ZnO/MWCNTs.

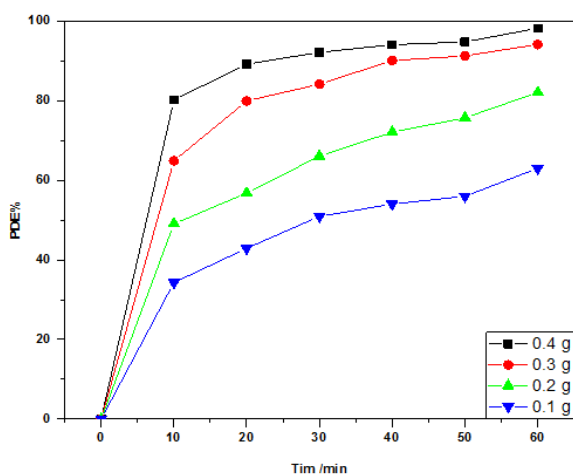


Figure 6. Effect of weight of ZnO/MWCNTs on PDE% by DY dye.

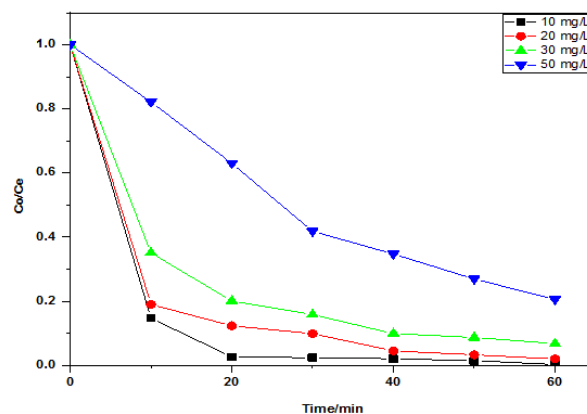


Figure 7. Impact of Photo degradation of ZnO/MWCNTs by DY dye

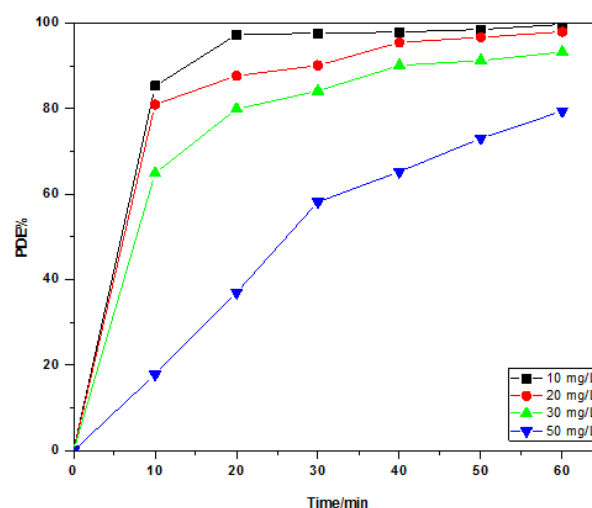


Figure 8. Effect several concentrations of DY dye onto (PDE%)

#### Effect concentration of DY dye

The impact of initial DY dye concentration under UV light utilized from 10-100 mg/L in the presence of 0.3 g of ZnO/MWCNTs, pH solution 5, and light intensity (1.27 mW/cm<sup>2</sup>). The data are demonstrated in Figure 7. The concentration of DY dye is determining factor in most of elimination of DY dye, especially in photocatalytic degradation. As the DY dye concentration raises, it prevents the penetration of light irradiation into the medium. Thus, DY dye PDE% would increase remarkably, it means that with greater concentration , the DY dye of the PDE% decreases [7-8,24-25].

In **Figure 8**, it is observed that the DY dye photo catalytic degradation (PDE%) rises as the concentration of DY dye decreases and the photo catalytic degradation increased from (93.67%-62.76%), and this occurs either by reducing holes or (OH) because the sites active will complete the coverage with the DY dye, or increase in the concentration caused an increased adsorption of the DY dye on to ZnO/MWCNTs, which leads to reduced (OH) radical generation, because that is low availability of the free active site on the surface [15,26].

## Conclusion


ZnO NPs was grafted onto the MWCNTs framework and then utilized for photo reduction of DY dye, and the ZnO NPs introduction heightened the absorption of solar light. Under solar light irradiation, nanocomposite can completely remove DY dye (30 mg/L) solution in 1 h. After that, the degradation study indicated that the effective DY dye removal from aqueous solutions was accomplished via nanocomposite, with the best degradation at concentration of 30 mg/L from adsorbent, and then improved photo catalytic performance of the produced ZnO/MWCNTs. Through the data, it was found that using nanocomposite significantly affect the photo degradation of DY dye leading to 95% photocatalytic degradation at 60 min.

## Conflict of interest


The authors declare that they have no conflict of interest

## Orcid

Thura Zayad Fathallah : 0009-0003-7242-2640

Youssef Ali Naeem : 0000-0002-0578-0996

Ameer Hassan Idan : 0000-0001-7276-469X

Hussein Ali Kadhim Kyhoiesh : 0000-0002-3830-6326

## References

- [1] A.S. Yusuff, B.A. Obende, T.C. Egbosiuba, Photocatalytic decolorization of textile effluent over ZnO nanoparticles immobilized on eucalyptus bark biochar: Parametric optimization, kinetic and economic analyses, *Water Resources and Industry*, **2024**, *31*, 100245. [[CrossRef](#)], [[Google Scholar](#)], [[Publisher](#)]
- [2] R. Syah, A.H. Altajer, O.F. Abdul-Rasheed, F.A. Tanjung, A.M. Aljeboree, N.A. Alrazzak, A.F. Alkaim, CuMoO<sub>4</sub>/ ZnO nanocomposites: Novel synthesis, characterization, and photocatalytic performance, *Journal of Nanostructures*, **2021**, *11*, 73-80. [[CrossRef](#)], [[Google Scholar](#)], [[Publisher](#)]
- [3] Reza K.M, Kurny A, Gulshan G, Parameters affecting the photocatalytic degradation of dyes using TiO<sub>2</sub>: A review, *Applied Water Science*, **2017**, *7*, 1569-1578. [[CrossRef](#)], [[Google Scholar](#)], [[Publisher](#)]
- [4] M. Irani, Photocatalytic degradation of methylene blue with ZnO nanoparticles; a joint experimental and theoretical study, *Journal of the Mexican Chemical Society*, **2026**, *3*, 1870-2490. [[Google Scholar](#)], [[Publisher](#)]
- [5] A.T. Jalil, H.E.A. Qurabiy, S.H. Dilfy, S.O. Meza, S. Aravindhana, M.M. Kadhim, A.M. Aljeboree, CuO/ZrO<sub>2</sub> nanocomposites: Facile synthesis, characterization and photocatalytic degradation of tetracycline antibiotic, *Journal of Nanostructures*, **2021**, *11*, 333-346. [[CrossRef](#)], [[Google Scholar](#)], [[Publisher](#)]
- [6] S.K. Jayaraj, V. Sadishkumar, T. Arun, P. Thangadurai, Enhanced photocatalytic activity of V2O5 nanorods for the photodegradation of organic dyes: A detailed understanding of the mechanism and their antibacterial activity, *Materials Science in Semiconductor Processing*, **2018**, *85*, 122-133. [[Crossref](#)], [[Google Scholar](#)], [[Publisher](#)]
- [7] M.S. Mashkour, A.F. Al-Kaim, L.M. Ahmed, F.H. Hussein, Zinc oxide assisted photocatalytic



- decolorization of reactive red 2 dye, *International Journal of Chemical Sciences*, **2011**, *9*, 969-979. [[Google Scholar](#)], [[Publisher](#)]
- [8] S. Halder, R. Dammalapati, B. Bhaduri, ZnO nanoparticles dispersed in nitrogen-enriched carbon matrix for the efficient adsorption and photocatalytic degradation of aqueous methylene blue molecules, *Inorganic Chemistry Communications*, **2023**, *158*, 111685. [[Crossref](#)], [[Google Scholar](#)], [[Publisher](#)]
- [9] S. Chkirida, N. Zari, R. Achour, H. Hassoune, A. Lachehab, R. Bouhfid, Highly synergic adsorption/photocatalytic efficiency of Alginate/Bentonite impregnated TiO<sub>2</sub> beads for wastewater treatment, *Journal of Photochemistry and Photobiology A: Chemistry*, **2021**, *412*, 113215. [[Crossref](#)], [[Google Scholar](#)], [[Publisher](#)]
- [10] A.M. S. S. Sambaza, and K. Pillay, Polyaniline-coated TiO<sub>2</sub> nanorods for photocatalytic degradation of bisphenol A in water, *ACS Omega*, **2020**, *5*, 29642-29656. [[Crossref](#)], [[Google Scholar](#)], [[Publisher](#)]
- [11] Z. Zhou, S. Lin, T. Yue, T.C. Lee, Adsorption of food dyes from aqueous solution by glutaraldehyde cross-linked magnetic chitosan nanoparticles, *Journal of Food Engineering*, **2014**, *126*, 133-141. [[Crossref](#)], [[Google Scholar](#)], [[Publisher](#)]
- [12] M.A.M. Salleh, D.K. Mahmoud, W.A.W.A. Karim, A. Idris, Cationic and anionic dye adsorption by agricultural solid wastes: A comprehensive review, *Desalination*, **2011**, *280*, 1-13. [[Crossref](#)], [[Google Scholar](#)], [[Publisher](#)]
- [13] A.M. Aljeboree, S.M. Essa, Z.M. Kadam, F.A. Dawood, D. Falah, A.F. Alkaim, Environmentally friendly activated carbon derived from palm leaf for the removal of toxic reactive green dye, *International Journal of Pharmaceutical Quality Assurance*, **2023**, *14*, 12-15. [[Crossref](#)], [[Google Scholar](#)], [[Publisher](#)]
- [14] M.A.A.H. Allah, H.A. Alshamsi, Green synthesis of AC/ZnO nanocomposites for adsorptive removal of organic dyes from aqueous solution, *Inorganic Chemistry Communications*, **2023**, *157*, 111415. [[Crossref](#)], [[Google Scholar](#)], [[Publisher](#)]
- [15] A. Nasser, B. Sina, A. Maryam, J. Saeedeh, A new method for preparing ZnO/CNT nanocomposites with enhanced photocatalytic degradation of malachite green under visible light, *Journal of Photochemistry and Photobiology A: Chemistry*, **2020**, *389*, 112207. [[Crossref](#)], [[Google Scholar](#)], [[Publisher](#)]
- [16] A. Sharma, R. Nagraik, S. Sharma, G. Sharma, S. Pandey, S. Azizov, P.K. Chauhan, D. Kumar, Green synthesis of ZnO nanoparticles using Ficus palmata: Antioxidant, antibacterial and antidiabetic studies, *Results in Chemistry*, **2022**, *4*, 100509. [[Crossref](#)], [[Google Scholar](#)], [[Publisher](#)]
- [17] Z.D. Alhattab, A.M. Aljeboree, M.A. Jawad, F.S. Sheri, A.K.O. Aldulaim, A.F. Alkaim Highly adsorption of alginate/bentonite impregnated TiO<sub>2</sub> beads for wastewater treatment: Optimization, kinetics, and regeneration studies, *Caspian Journal of Environmental Sciences*, **2023**, *21*, 657-664. [[Crossref](#)], [[Google Scholar](#)], [[Publisher](#)]
- [18] B. Maryam, A. Murrawat, A. Naeem, J. Sofia, A.S. Nazar, Synthesis of ZnO/CNT nanocomposites for ultraviolet sensors, *Frontiers in Materials*, **2022**, *9*, 835521. [[Crossref](#)], [[Google Scholar](#)], [[Publisher](#)]
- [19] A. Norouzi, A. Nezamzadeh-Ejhieh, Designing the photodegradation experiments of a dye polluted water by  $\alpha$ -Fe<sub>2</sub>O<sub>3</sub>/Cu<sub>2</sub>O and the mechanism study, *Materials Chemistry and Physics*, **2023**, *305*, 127918. [[Crossref](#)], [[Google Scholar](#)], [[Publisher](#)]
- [20] J.N. Sahu, J. Acharya, B.C. Meikap, Optimization of production conditions for activated carbons from Tamarind wood by

- zinc chloride using response surface methodology, *Bioresource Technology*, **2010**, *101*, 1974-1982. [[Crossref](#)], [[Google Scholar](#)], [[Publisher](#)]
- [21] N.A.-H. Baiee, A.F. Alkaim, Photocatalytic degradation of methylene blue dye from aqueous solutions in the presence of synthesized ZnO nanoparticles, *NeuroQuantology*, **2021**, *19*, 53. [[Crossref](#)], [[Google Scholar](#)], [[Publisher](#)]
- [22] T.G. Yan, W. Jingyu, X. Ganghua, L.Z. Haiming, Degradation of sulfadiazine in aqueous media by peroxymonosulfate activated with biochar-supported ZnFe<sub>2</sub>O<sub>4</sub> in combination with visible light in an internal loop-lift reactor, *Yan Wang, ORCID logo a Tao Gan, a Jingyu Xiu, a Ganghua Liua and Haiming Zou*, **2022**, *2*, 22-29. [[Crossref](#)], [[Google Scholar](#)], [[Publisher](#)]
- [23] Z. Mirzaeifard, Z. Shariatnia, M. Jourshabani, S.M. Rezaei Darvishi, ZnO photocatalyst revisited: effective photocatalytic degradation of emerging contaminants using S-doped ZnO nanoparticles under visible light radiation, *Industrial & Engineering Chemistry Research*, **2020**, *59*, 15894-15911. [[Crossref](#)], [[Google Scholar](#)], [[Publisher](#)]
- [24] T.S. Wu, K.X. Wang, G.D. Li, S.Y. Sun, J. Sun, J.S. Chen, Montmorillonite-supported Ag/TiO<sub>2</sub> nanoparticles: An efficient visible-light bacteria photodegradation material, *ACS Applied Materials & Interfaces*, **2010**, *2*, 544-550. [[Crossref](#)], [[Google Scholar](#)], [[Publisher](#)]
- [25] Y. Ma, N. Gao, C. Li, Degradation and pathway of tetracycline hydrochloride in aqueous solution by potassium ferrate, *Environmental Engineering Science*, **2012**, *29*, 357-362. [[Crossref](#)], [[Google Scholar](#)], [[Publisher](#)]
- [26] R. Mohamed, M. Barakat, Enhancement of photocatalytic activity of ZnO/SiO<sub>2</sub> by nanosized Pt for photocatalytic degradation of phenol in wastewater, *International Journal of Photoenergy*, **2012**, *2012*, 103672. [[Crossref](#)], [[Google Scholar](#)], [[Publisher](#)]

#### HOW TO CITE THIS ARTICLE

R. Abdulamer, T.Z. Fathallah, R. Sattar, Y.A. Naeem, A.H. Idan, H.A.K. Kyhoiesh, Y.M. Nasr. Enhanced Photocatalytic Removal of Direct Yellow 50 by ZnO/MWCNTs Nanocomposite under Solar Light Irradiation through Response Surface Methodology (RSM) Optimization. *Adv. J. Chem. A*, 2025, 8(1), 97-106.

DOI: [10.48309/AJCA.2025.465609.1580](https://doi.org/10.48309/AJCA.2025.465609.1580)

URL: [https://www.ajchem-a.com/article\\_202336.html](https://www.ajchem-a.com/article_202336.html)